



PAPER ID: 10A120



## DETERMINATION OF SUB-SOIL SHEAR WAVE VELOCITY ( $\bar{V}_S^{30}$ ) IN LAYERED SOIL WITH FEM IN RELATION TO APPROXIMATED AND ANALYTICAL RESULTS

Masoud Motalebian <sup>a</sup>, Masoud Hajjalilue Bonab <sup>b\*</sup>, Mohammad Davoudi <sup>c</sup>

<sup>a</sup> Department of Civil Engineering, Science and Research Branch, Islamic Azad University, Tehran, IRAN.

<sup>b</sup> Department of Civil Engineering, University of Tabriz, Tabriz, IRAN.

<sup>c</sup> International Institute of Earthquake Engineering and Seismology, Tehran, IRAN.

### ARTICLE INFO

#### Article history:

Received 08 April 2019  
Received in revised form 19 July 2019  
Accepted 30 July 2019  
Available online 07 August 2019

#### Keywords:

Iranian Code of Practice; Standard2800; Modal Analysis; FEM; Evolutionary Polynomial Regression (EPR); Numerical geotechnical analysis; Two-layered soil profile; Three-layered soil profile.

### ABSTRACT

Determining the shear wave velocity of subsoil ( $V_s$ ) is one of the important parameters in the seismic design of structures. To determine the equivalent shear wave velocity in layered soil ( $\bar{V}_S$ ), several approximated relations and, in some cases, analytical ones have been proposed. The present study aims to determine the equivalent shear wave velocity in the top 30 meters ( $\bar{V}_S^{30}$ ) in single layer soil with variable shear modulus, and also in two- and three-layered soil using numerical analysis. For the numerical investigation, ABAQUS based on finite element method (FEM) was used and modal analysis was performed by calculating the eigenvalues. The obtained values were compared with analytical and other approximated relations including the presented relation by the Iranian Code of Practice for Seismic Resistant Design of Buildings (Standard2800). The results show that, when the upper layers have smaller  $V_s$  than that of the lower layers, Standard2800 relation presents smaller values than that of the numerical results for the  $\bar{V}_S^{30}$ . Also, when the lower layers have smaller  $V_s$  than that of the upper layers, Standard2800 relation presents larger values. Also, an absolute agreement was observed between numerical and analytical results and Standard2800 relation has better consistency with numerical and analytical results compared with other similar cases. In addition, Evolutionary Polynomial Regression (EPR) was used to derive an accurate model expressing  $\bar{V}_S^{30}$  in terms of dimensionless parameters in two-layered soil.

© 2019 INT TRANS J ENG MANAG SCI TECH.

## 1. INTRODUCTION

It is obviously recognized that the effect of the site is the most important characteristic of ground motion and has a well-known influence on the earthquake damage. During an earthquake, the ground motion traits of the site are specifically affected by the soil deposits (Maheswari et al. 2008, Trifunac et al. 2016). Shear wave velocity of soil ( $V_s$ ) is regarded as the main parameter for site classification and

evaluation of earthquake hazard because of its great effect on the local ground motion amplification (Seshunarayana & Sundararajan 2012).  $V_s$  has long been known as being a fundamental parameter for considering the dynamic properties of soil and representing the stiffness of the soil layers and its relation to the amplification of the ground (Roy and Sahu 2012).

In current engineering practice, consideration of the equivalent shear wave velocity ( $\bar{V}_s$ ) is implemented by using different design spectra for different site classes specified in seismic codes (Street et al. 1997). A variety of approximated relations have been proposed in order to determine  $\bar{V}_s$  in uniformed layered soil with a different height ( $H_i$ ), shear wave velocity ( $V_{s_i}$ ), and density ( $\rho_i$ ) that overlying the rigid bedrock according to Figure 1 (Sawafa, 2004).

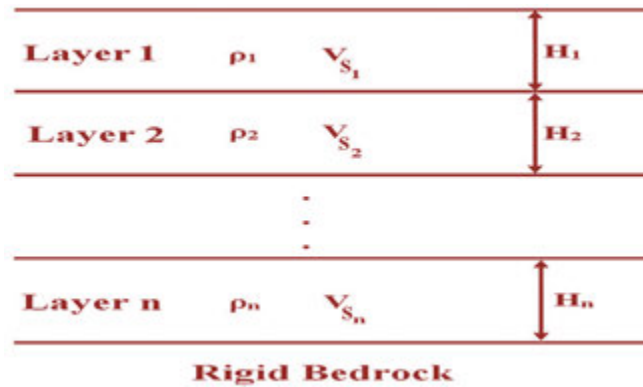


**Figure 1:** Soil layers with different height, shear wave velocity, and specific mass (Sawafa, 2004)

One of the recognized but simple relations soil is the identification of  $\bar{V}_s$  based on the weighted average of natural periods of different layers by Eq. 1 (Mohamed et al 2013).

$$\bar{V}_s = \frac{\sum_{i=1}^n \Sigma(H_i)}{\sum_{i=1}^n \Sigma(H_i / V_{s_i})} \quad (1)$$

This approximated relation has been used to determine  $\bar{V}_s$  in most of the codes for the seismic design of buildings including UBC97 (1997), IBC (2006), EuroCode08 (2008), NEHRP (2009), NBCC (2011), and also Iranian Code of Practice for Seismic Resistant Design of Buildings (Standard2800) (2014). Based on this relation, the arrangement of soil layers is not important for the calculation of the  $\bar{V}_s$ . In the Iranian Code of Practice for Seismic Resistant Design of Buildings (Standard 2800), based on  $\bar{V}_s$  in the top 30 meters of site ( $\bar{V}_s^{30}$ ), soil can be classified into I, II, III and IV types in regard to Table 1.

**Table 1:** Soil types based on  $\bar{V}_s^{30}$  (Standard2800, 2015)

Soil profile type	$\bar{V}_s^{30}$ (m/sec)
I	$\bar{V}_s^{30} > 750$
II	$375 < \bar{V}_s^{30} \leq 750$
III	$175 < \bar{V}_s^{30} \leq 375$
IV	$\bar{V}_s^{30} \leq 175$

Among those approximated relations used for determining  $\bar{V}_s$ , the method of the weighted average of the shear wave velocity of soil layers (WAV) (Madera, 1971) can be calculated based on

$$\bar{V}_S = \frac{1}{\sum_{i=1}^n H_i} \sum_{i=1}^n V_{S_i} H_i \quad (2).$$

This approximated relation has been used in Building Japanese Code (Estrada, 2004).

Another approximated relation used for determining  $\bar{V}_S$  is based on the method of the weighted average of the shear wave velocity of soil layers (WAV) (Vijayendra et al. 2015) can be calculated by

$$\bar{V}_S = \sqrt{\frac{\bar{G}_s}{\bar{\rho}_s}} \quad (3),$$

where  $\bar{G}_s$  and  $\bar{\rho}_s$  are the equivalent shear modulus and the equivalent density of soil, which can be determined by Equations (4) and (5), respectively.

$$\bar{G}_s = \frac{1}{\sum_{i=1}^n H_i} \sum_{i=1}^n G_{S_i} H_i \quad (4).$$

$$\bar{\rho}_s = \frac{1}{\sum_{i=1}^n H_i} \sum_{i=1}^n \rho_{s_i} H_i \quad (5).$$

The term  $G_{S_i}$  is the shear modulus of each layer.

## 2. FINITE-ELEMENT MODELING AND BASELINE ANALYSIS MODEL

The present study aims to estimate the numerical value of the  $\bar{V}_S^{30}$  and compare the values obtained from the relation proposed by Standard2800 (Eq. 1) for different soil layers. In some cases, some analytical relations have been presented by researchers, which were also compared in order to give better validation. Moreover, the results obtained from the approximated methods including WAM and WAV were compared with the numerical and analytical results. Also, Evolutionary Polynomial Regression (EPR) is used to derive an equation indicating  $\bar{V}_S^{30}$  in terms of dimensionless parameters for two-layered soil.

For numerical investigation of the problem, finite elements software ABAQUS 6.12-3 was used. The modal analysis was conducted by calculating the eigenvalues. Accordingly, the fundamental period of the site including different layers ( $\bar{T}$ ) can be determined and the required  $\bar{V}_S$  can be estimated by Eq. 6 (Roser and Gosar, 2010).

$$\bar{V}_S = \frac{4H}{\bar{T}} \quad (6).$$

Parameter H is the total height of all the layers. In all the investigated cases in this paper, the total height of the layers is assumed 30m and overlying rigid bedrock.

This research was conducted based on a two-dimensional model (plane strain). According to the modal analysis, soil behavior was assumed as a linear elastic one. Figure 2a shows the meshed model of the three-layered soil that is developed for modal analysis and the first vibration mode and the

corresponding frequency (output of FE) are illustrated in Figure 2b.

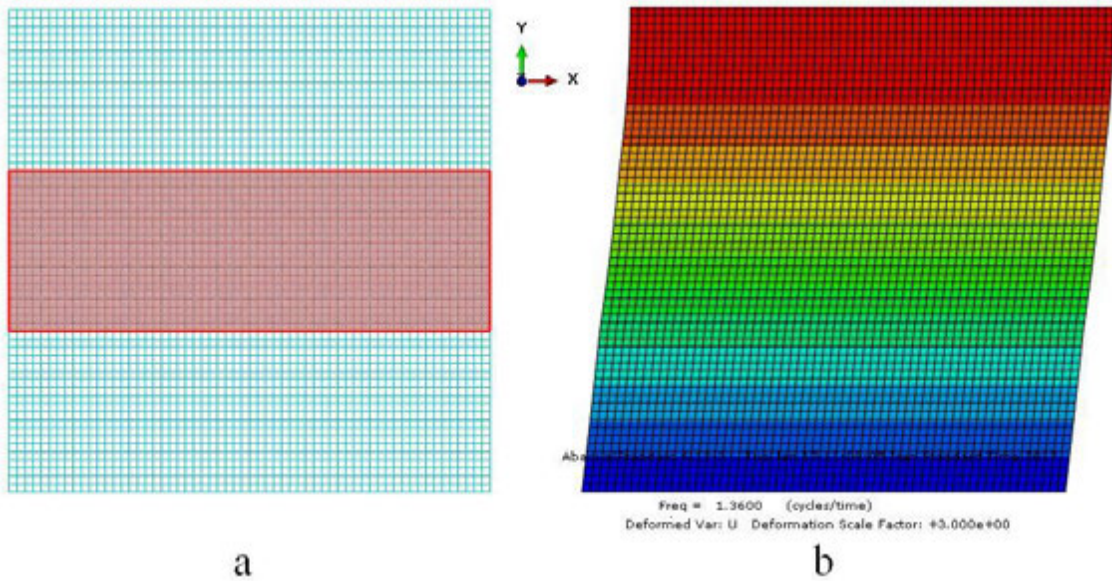


**Figure 2** a) A three-layered uniform soil layer; meshed in ABAQUS (plane strain)  
 b) First vibration mode (along axis-x) obtained from the modal analysis

In the following different layers, arrangements were illustrated and the numerical and analytical results were compared with Standard2800 and the other approximated and analytical relations.

### 3. $\bar{V}_s^{30}$ IN A SINGLE-LAYERED SOIL WITH LINEAR VARIATIONS IN THE SOIL SHEAR MODULUS

In a soil layer with height  $H$  overlying rigid bedrock with linear variations of shear modulus in which the shear modulus of soil in upper and lower layers are  $G_0$  and  $G_H$ , respectively,  $\bar{V}_s$  is equal to the shear wave velocity of the soil at the depth of  $Z_{eq}$ . Based on Dobry et al. (1976) results,  $Z_{eq}$  can be calculated by the results of the partial Bessel's equations based on  $K$  value or according to Figure 3 ( $K = \sqrt{G_0/G_H}$ ).  $K > 1.0$  represents the decrease, while  $K < 1.0$  represents the increase in the shear modulus at the depth of soil.

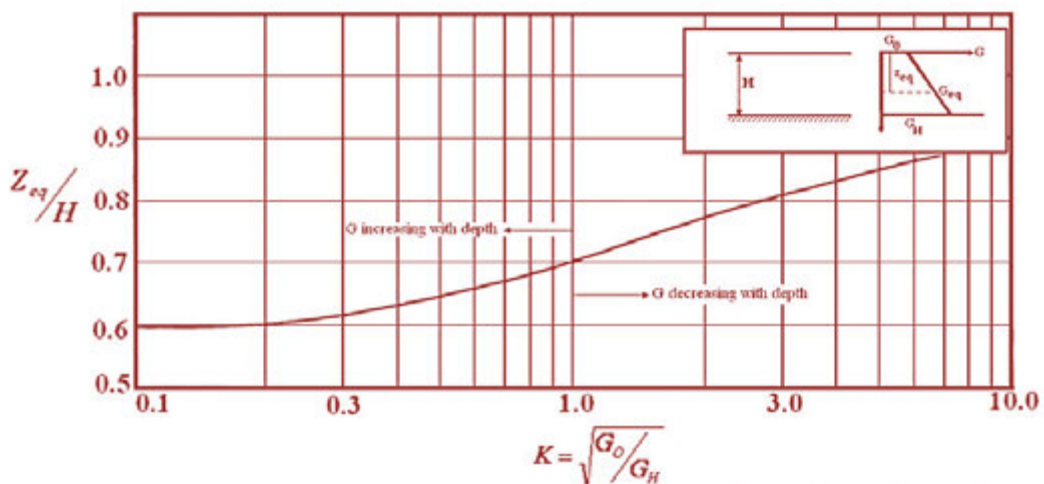


**Figure 3:** Determining the equivalent depth for the soil with linear variations of shear modulus in depth (after Dobry et al. (1976)).

Although the relation proposed by the Standard2800 does not include in this case, VS of each layer

can be calculated and  $\bar{V}_S$  can be estimated through the stairway classification of soil into several layers. To this end, the soil with 30m high and linear variable shear modulus consists of 10 layers with 3m high is considered and  $\bar{V}_S^{30}$  is estimated based on the Standard2800. The same process is also carried out in numerical modeling. For different K values, the equivalent depth ratio ( $Z_{eq}/H$ ) is compared based on the analytical and numerical methods, Standard2800 relation, WAM and WAV methods in Figure 4.

The results show an appropriate agreement between numerical and analytical results. Minor differences between the results could be related to the linear variations of the shear modulus in the analytical method and the stairway variations in the numerical modeling. The proposed relation by Standard2800 predicts the equivalent depth, particularly due to the increase in the shear modulus at depth which is not significantly lower than the obtained results of the numerical and analytical methods.

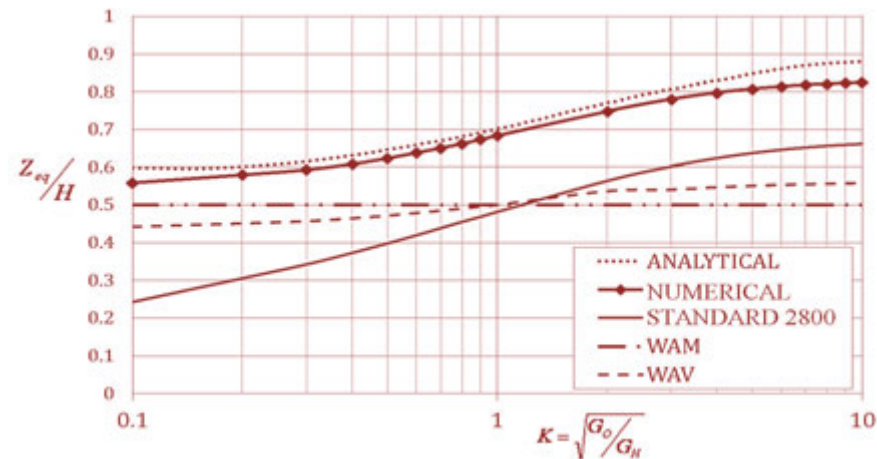


**Figure4:**  $Z_{eq}/H$  with linear variations of shear modulus by different methods.

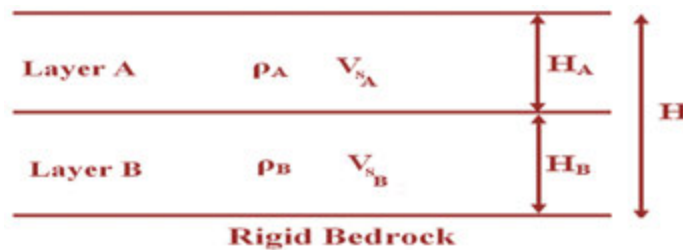


**Figure 5:** Soil profile with two different uniformed layers ( $\rho_A=\rho_B$ ).

#### 4. $\bar{V}_S^{30}$ IN TWO-LAYERED SOIL

According to the analytical results the fundamental period ( $\bar{T}$ ) for a site consisting of two layers A and B located on the rigid bedrock (Figure 5), with height and shear wave velocity of  $H_A$ ,  $H_B$ , and  $V_{sA}$ ,  $V_{sB}$  respectively, can be calculated by Equation (7) (Oskay and Zeghal, 2011).

$$\tan\left(\frac{\pi T_A}{2 \bar{T}}\right) \tan\left(\frac{\pi T_B}{2 \bar{T}}\right) = \frac{H_B T_A}{H_A T_B} \quad (7),$$

where  $T_A = \frac{4H_A}{V_A}$  and  $T_B = \frac{4H_B}{V_B}$  are respectively the fundamental period of layers A and B, in the absence of other layers, and  $\bar{T}$  is the fundamental period of the two-layered soil, respectively. Having  $\bar{T}$  from the above equation and given Equation (6),  $\bar{V}_S^{30}$  can be calculated using Equation (8).

$$\tan\left(\frac{\bar{V}_S^{30} \pi}{2V_{sA}} \frac{H_A}{H_A + H_B}\right) \tan\left(\frac{\bar{V}_S^{30} \pi}{2V_{sB}} \frac{H_B}{H_A + H_B}\right) = \frac{V_{sB}}{V_{sA}} \quad (8),$$

where  $H_A + H_B = H = 30\text{m}$ . Results obtained by the numerical method, analytical methods, the relation proposed by the Standard2800, and other approximated methods are calculated and compared for a two-layered soil for the following cases. Finally, Evolutionary Polynomial Regression (EPR) was used to derive an accurate equation expressing  $\bar{V}_S^{30}$  in terms of dimensionless parameters. These results are based on  $V_{SA} = 200\text{m/s}$  and can be generalizable for other dimensionless ratios.

#### 4.1 A WEAK SOIL LAYER ON A STRONG LAYER WITH VARIABLE HEIGHT

In this case, two soil layers with different heights with the total height of 30m were considered and the effect of  $\frac{H_A}{H_A + H_B}$  on  $\frac{\bar{V}_S^{30}}{V_{SA}}$  was investigated. Also, it was assumed that  $V_{SA} = 0.2V_{SB}$ .

The results (Figure 6) showed Standard2800 which produced lower values for  $\bar{V}_S^{30}$ , especially for lower values of the ratio  $\frac{H_A}{H_A + H_B}$ . Moreover, there was an absolute agreement between results of the numerical finite element method and the results of analytical analysis. The approximated relation in Standard2800 had better consistency with the analytical results compared to the approximated methods of WAM and WAV.

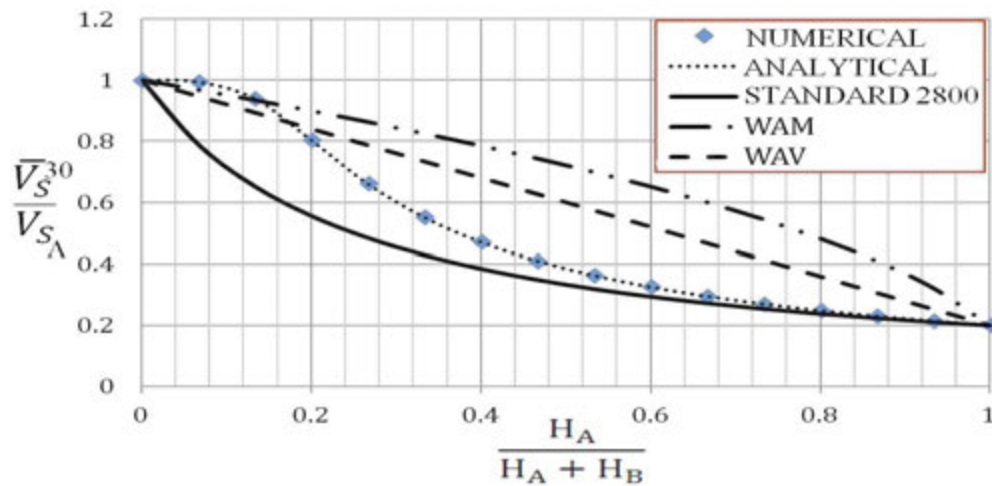


**Figure 6:**  $\frac{\bar{V}_S^{30}}{V_{SA}}$  with variable height.

#### $H_A = H_B = 15\text{m}$ and $V_{SB} = \alpha \times V_{SA}$

Results obtained for  $\frac{\bar{V}_S^{30}}{V_{SA}}$  showed that for  $\alpha > 1.0$  (the weak layer on top), the Standard2800 provided lower values for the ratio of  $\bar{V}_S^{30}$  than those provided by analytical and numerical results and, for  $\alpha < 1.0$  (the weak layer in the bottom), the Standard2800 would result in higher values than those for the analytical and numerical results. Also, the numerical results were completely in agreement with the analytical results and the approximated relation proposed by the standard2800 had better consistency compared to the approximated methods of WAV and WAM. (Figure 7).

#### $H_A = 10\text{m}$ , $H_B = 20\text{m}$ and $V_{SB} = \alpha \times V_{SA}$

The findings for  $\frac{\bar{V}_S^{30}}{V_{SA}}$  were in line with those of the previous case, however, the difference between the results of the Standard2800 relation and the numerical analysis as well as analytical results were more obvious for  $\alpha > 1.0$  (Figure 8). In the present case, the approximated relation in the Standard2800 had better consistency compared to the approximated WAV and WAM methods.

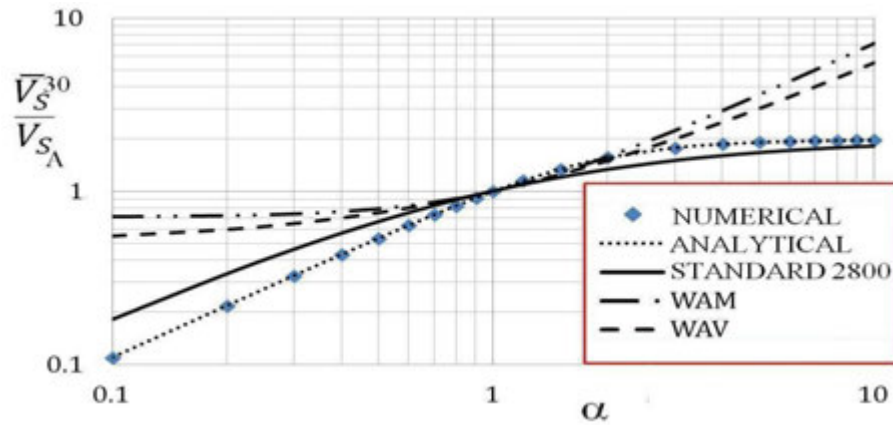


**Figure 7**  $\frac{\overline{V_S^{30}}}{V_{S_A}}$  for  $H_A=H_B$  and different values of  $\alpha$ .

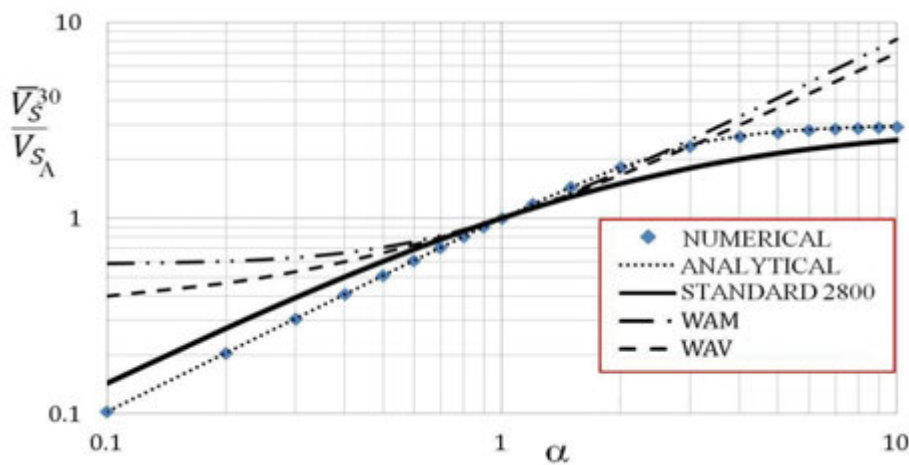


**Figure 8:**  $\frac{\overline{V_S^{30}}}{V_{S_A}}$  for  $H_A=0.5H_B$  and different values of  $\alpha$ .

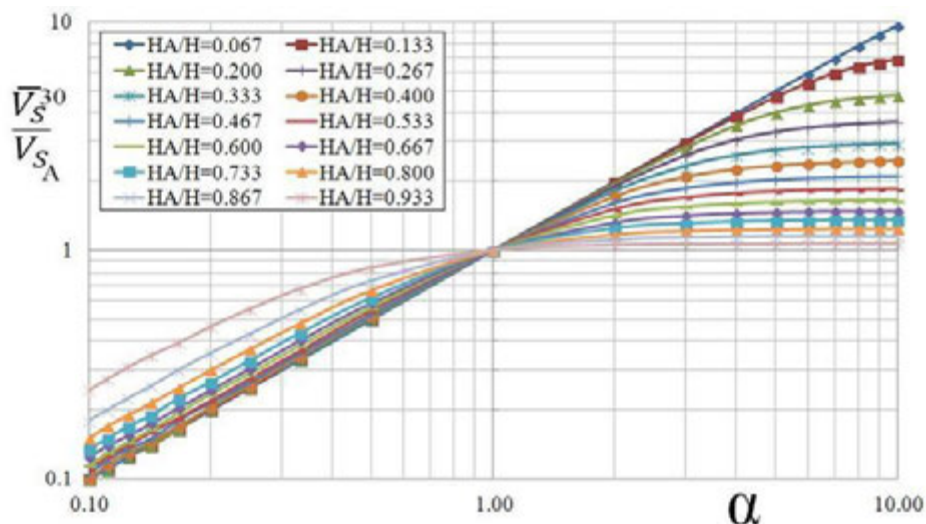


**Figure 9:**  $\frac{\overline{V_S^{30}}}{V_{S_A}}$  for different values of  $\alpha$  and  $H_A/H$

#### 4.2 $\overline{V_S^{30}}$ IN TWO LAYERED SOIL WITH EPR MODELLING

Equation (8) is a closed-form equation and  $\overline{V_S^{30}}/V_A$  can be determined using Figure 9, directly.

Based on Figure 9,  $\frac{\overline{V_S^{30}}}{V_{S_A}}$  can be expressed with a relation in terms of two dimensionless variables of  $\alpha$

and  $H_A/H$ . This relation was derived using the Evolutionary Polynomial Regression (EPR). This technique uses multi-objective genetic programming to derive regression equations by creating symbolic models (Giustolisi and Savic, 2006). This technique was originally used for modeling environmental phenomena, but later found applications in geotechnical engineering for predicting and evaluating surface settlement (Rezania and Javadi, 2007), soil permeability characteristics and soil compressibility (Ahangar-Asr et al. 2011) and liquefaction potential of sand (Shahnazari et al, 2013). In this study, the problem was modeled using a software application with the EPR name, which has been coded in MATLAB (Giustolisi and Savic, 2006).

When developing the model, two-thirds of the 270 available data instances were randomly chosen to operate as training data and the remaining one-third was used as test data. This EPR modeling yielded Equation (9), which expresses  $\frac{\bar{V}_S^{30}}{V_{S_A}}$  as a function of dimensionless parameters of  $\alpha$  and  $H_A/H$ .

$$\frac{\bar{V}_S^{30}}{V_{S_A}} = e^{0.78 \times \sqrt[4]{\frac{\alpha}{(H_A/H)^{-0.4}}} - 1} \quad (9)$$

where  $e$  is Euler's number. To examine the performance of the chosen model, statistical measures including the correlation coefficient ( $R$ ), the slope of the regression line in the plot of actual against predicted values ( $k$ ), and the slope of the regression line in the plot of predicted against actual values ( $k'$ ) were investigated.  $R$ ,  $k$  and  $k'$  obtained from Eq. 10 to 12, respectively. These values are presented in Table 2 for training and test data (Rashed et al 2011).

$$R = \frac{\sum_{i=1}^N (h_i - \bar{h}_i)(t_i - \bar{t}_i)}{\sqrt{\sum_{i=1}^N (h_i - \bar{h}_i)^2 \sum_{i=1}^N (t_i - \bar{t}_i)^2}} \quad (10)$$

$$k = \frac{\sum_{i=1}^N (h_i \times t_i)}{\sum_{i=1}^N h_i^2} \quad (11)$$

$$k' = \frac{\sum_{i=1}^N (h_i \times t_i)}{\sum_{i=1}^N t_i^2} \quad (12)$$

Where  $h_i$  and  $t_i$  are, respectively, the numerical and predicted results for data instance  $i$ ;  $\bar{h}_i$  and  $\bar{t}_i$  are the mean values of numerical and predicted results, and  $N$  is the number of samples. The closer  $R$ ,  $k$  and  $k'$  the values close to 1, the higher the accuracy of model predictions (Rashed et al 2011) is. Based on a rational hypothesis, Smith (1986) has suggested that  $|R| > 0.8$  indicates strong proximity between actual and predicted values. Golbraikh and Tropsha (2002) have suggested that for a model to be suitable, either  $k$  or  $k'$  should be between 0.85 and 1.15. As seen in Table 2, the results obtained for training and test data show acceptable proximity, which reflects the suitable accuracy of the derived



equation.

**Table 2:** Evaluation of  $\frac{\bar{V}_S^{30}}{V_{SA}}$  estimation model

Data Type	Number number	k'	k	R
Trained	180	1.0462	0.9135	0.9744
Tested	90	1.0587	0.9138	0.9594
All	270	1.0507	0.9136	0.9654

## 5. $\bar{V}_S^{30}$ IN THREE-LAYERED SOIL

In this case, three layers with the height of 10m were modeled and the shear wave velocity of upper, middle, and lower layers was assumed to be  $\frac{V_s}{\alpha}$ ,  $V_s$ , and  $\alpha \times V_s$ , respectively (Figure 10). According to Figure 11, the results showed that, for  $\alpha > 1.0$  (increase in the  $V_s$  in the lower layers), the Standard2800 presented lower values for the  $\bar{V}_S^{30}$  and, for  $\alpha < 1.0$  (decrease in the  $V_s$  in lower layers), the Standard2800 presented higher values. Based on the Standard2800, an arrangement of the layers had no effect on the  $\bar{V}_S$  and the values would be equal to  $\alpha = 0.5$  and  $\alpha = 2.0$ . This assumption was not valid for the numerical results.

Also, the results obtained through WAM and WAV methods had significant and marked differences compared to those of the numerical results. These results are based on  $V_s = 200\text{m/s}$  and can be generalizable for other dimensionless ratios.



**Figure 10:** A three-layered uniformed soil with different shear wave velocity.

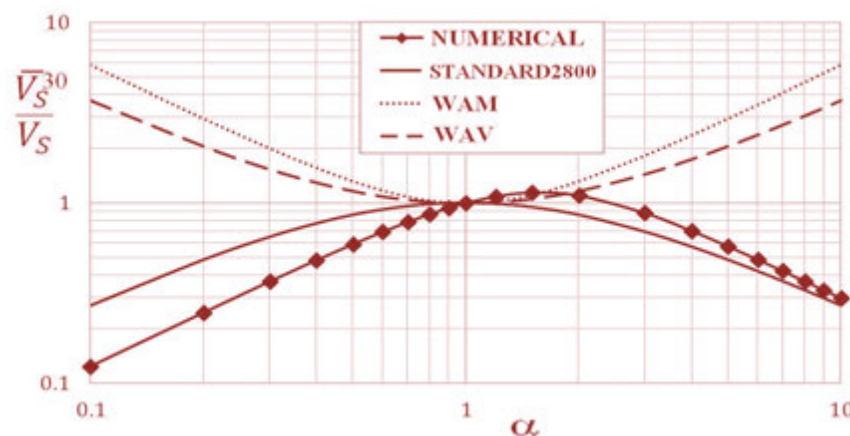


**Figure 11:**  $\frac{\bar{V}_S^{30}}{V_S}$  for different values of  $\alpha$ .

## 6. $\bar{V}_S^{30}$ IN A WEAK SOIL LAYER BETWEEN A STRONG LAYER

In this case, according to Figure 12, a soil layer with the height of  $H = 30\text{m}$  and shear wave velocity of  $V_S$  was assumed in which a weak layer with a height of  $2\text{m}$  and shear wave velocity of  $0.1V_S$  was located. In this condition, the effect of depth of the weak layer ( $H_1$ ) was investigated on the soil. According to the Standard2800, apart from the depth of this weak layer, the equivalent shear wave

velocity in the top 30 meters was equal to  $\bar{V}_S^{30} = 0.625V$ . It represented  $\bar{V}_S^{30} = 0.940V$  and  $\bar{V}_S^{30} = 0.966V$  for WAV and WAM methods, respectively. However, the obtained numerical results revealed that  $\frac{\bar{V}_S^{30}}{V_S}$  decreases with an increase in  $\frac{H_1}{H}$  (Figure 13). To put simply, when the weak layer was near the surface of the ground, the numerical results led to lower values, while in the case in which the weak layer was at the depth of the soil, the results presented higher values for the  $\bar{V}_S^{30}$ . Also, WAV and WAM methods produced higher values for the  $\bar{V}_S^{30}$ . These results are based on  $V_S=200\text{m/s}$  and can be generalizable for other dimensionless ratios.

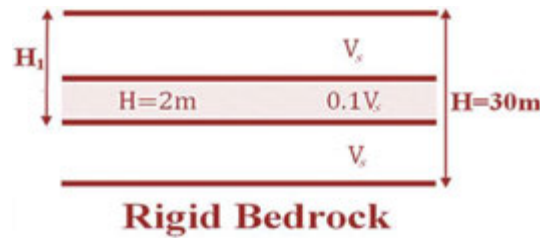


**Figure 12:** A weak layer in the middle of the strong layer.

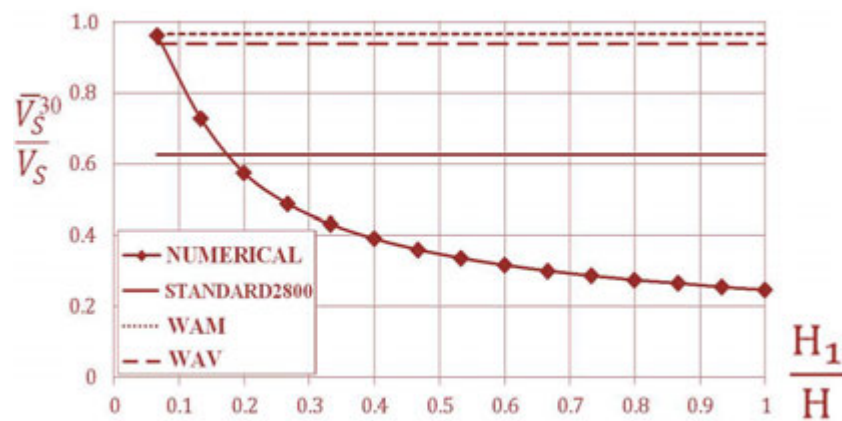


**Figure 13:**  $\frac{\bar{V}_S^{30}}{V_S}$  for different values of  $\frac{H_1}{H}$ .

## 7. $\bar{V}_S^{30}$ IN THREE-LAYERED SOIL PROFILE WITH DIFFERENT ARRANGEMENTS

In order to investigate the soil arrangement in  $\bar{V}_S^{30}$  in regard to Figure 14, three-layered soil profile with 3 various arrangements a, b, and c was modeled. The only existed difference between these three cases was an alteration in arrangement of them. Also, the height of each layer was assumed 10m in all cases. According to standard2800, in each case  $\bar{V}_S^{30} = 284 \text{ m/s}$  and in these three cases, the site is TYPE III (Table 3). However, based on the findings of numerical analysis,  $\bar{V}_S^{30}$  was distinct for every type and presented different site types for each of them. In line with the results obtained from numerical analysis, to what extent a softer layer was in the depth of soil,  $\bar{V}_S^{30}$  would provide lower value.

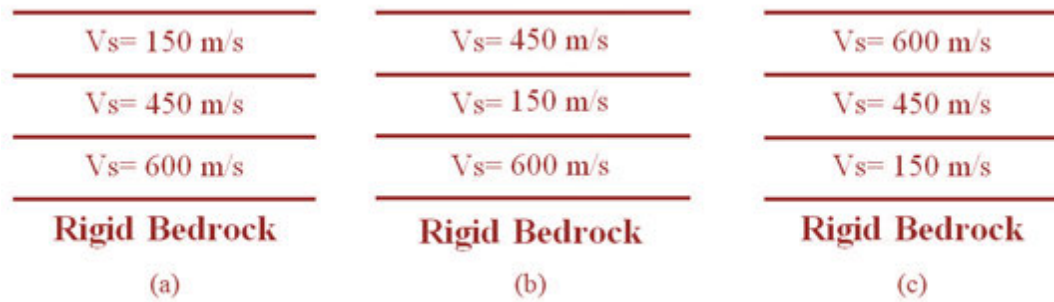


**Figure 14:** Three-layered soil profile with different arrangements.

**Table 3.** comparing the  $\bar{V}_S^{30}$  based on Standard2800 and numerical results

Case	Standard2800 (Equation (1))		Numerical	
	$\bar{V}_S^{30}$ (m/s)	Ground Type	$\bar{V}_S^{30}$ (m/s)	Ground Type
<b>a</b>	284	III	378	II
<b>b</b>	284	III	230	III
<b>c</b>	284	III	173	IV

## 8. CONCLUSION

The numerical investigation of the conducted research for determining  $\bar{V}_S^{30}$  based on the finite element method and the comparison with the proposed relation by Standard2800, analytical results, and other approximated methods showed that:

- In soil with linear variable shear modulus, comparison of the results obtained from the analytical method and the proposed relation by most of the building codes including Standard2800 indicated a significant difference in the  $\bar{V}_S^{30}$  values, particularly for increasing high linear variations in the shear modulus.
- For a two- (three-) layered soil where the Vs increased in low layer(s),  $\bar{V}_S^{30}$  obtained from Standard2800 was lower than that of the numerical and analytical results. But, by assuming a decrease in Vs in the lower layers, the proposed relation in Standard2800 presented lower values for  $\bar{V}_S^{30}$  than that of the numerical and analytical results.
- For the case when a weak soil layer was assumed, according to the Standard2800, the depth of this layer had no effect on  $\bar{V}_S^{30}$ . But, the numerical results showed that the closer this layer was to the surface, the higher the  $\bar{V}_S^{30}$  would be shown and location of this layer at the depth of the ground would decrease  $\bar{V}_S^{30}$ . A comparison of the numerical results with the values obtained from the relation in the Standard2800 showed a significant difference in this case.
- Although approximated methods of determining  $\bar{V}_S^{30}$  using the weighted average of shear wave velocity (WAV) and modulus (WAM) have relatively simple relations, same as the weighted average of periods (proposed relation in Standard2800), this relation had better consistency with numerical and analytical results in above cases.
- In this paper, a complete agreement was observed between the numerical and analytical results. The only minor difference was observed in the soil with variable shear modulus, which could be attributed to the linear variations of the shear modulus in the analytical method and the stairway variations in the numerical method. Obviously, it is possible to achieve a complete agreement between the numerical and analytical results by increasing the number of layers in this case.

Evolutionary Polynomial Regression (EPR) was used to derive an equation expressing  $\bar{V}_S^{30}$  in terms of dimensionless parameters for two-layered soil. The statistical measures showed an acceptable

correlation for the derived model.

## 9. AVAILABILITY OF DATA AND MATERIAL

Relevant information is available by contacting the corresponding author.

## 10. REFERENCES

- Ahangar-Asr. A., Faramarzi., A. Mottaghifard. and Javadi. A.A. (2011). Modeling of Permeability and Compaction Characteristics of Soils Using Evolutionary Polynomial Regression. *Computers and Geosciences*, 37(11), 1860-1869.
- Dobry, R., Oweis, I., Urzua, A. (1976). Simplified Procedure for Estimating the Fundamental Period of a Soil Profile. *Bulletin of the Seismological Society of America*, 66(4), 1293-1321.
- Estrada, G. (2004). Analysis Of Earthquake Site Response And Site Classification For Seismic Design Practices. *Proceeding of the 5th World Conference on Conference on Recent Advances in Geotechnical Earthquake Engineering and Soil Dynamics*, San Diego.
- Eurocode08. (2008). Seismic Design of Buildings Worked examples, European Commission Joint Research Centre; Ispra, Italy.
- Giustolisi. O. and Savic. D. (2006). A Symbolic Data-Driven Technique Based on Evolutionary Polynomial Regression. *Journal of Hydroinformatics*, 8(3), 207-222.
- Golbraikh. A. and Tropsha. A. (2002). Beware of  $q^2!$ . *Journal of Molecular Graphics and Modelling*, 20(4), 269–276.
- IBC (2006), International Building Code. International Code Council; Illinois, USA.
- Madera, G. A. (1971). Fundamental Period and Amplification of Peak Acceleration in Layered Systems. Report No. R70-37; Department of Civil Engineering, Massachusetts Institute of Technology, Cambridge, USA.
- Maheswari, U., Boominathan, A. and Dodagoudar, G. (2008). Development of Empirical Correlation Between Shear Wave Velocity and Standard Penetration Resistance in Soils of Chennai City. *Proceeding of the 14th World Conference on Earthquake Engineering*, Beijing, China, October.
- Mohamed. A., Abuelata, A., Abdelazim. F. and Tahaa. M. (2013). Site-specific shear wave velocity investigation for geotechnical engineering applications using seismic refraction and 2D multi-channel analysis of surface waves. *NRIAG Journal of Astronomy and Geophysics*, 2(1), 88-101.
- NBCC. (2011). National Building Code of Canada, National Research Council Canada; Ottawa Canada.
- NEHRP. (2009). National Earthquake Hazards Reduction Program, Recommended Seismic Provisions for Seismic Regulations for New Buildings and Other Structures. Building Seismic Safety Council of the National Institute of Building Sciences; Washington, USA.
- Oskay, C. and Zeghal, M. (2011). A survey of geotechnical system identification techniques. *Soil Dynamics and Earthquake Engineering*, 31(4), 568–582.
- Rashed, A., Bolouri. B. and Alavi. H. (2011). Nonlinear modeling of soil deformation modulus through LGP-based interpretation of pressuremeter test results. *Engineering Applications of Artificial Intelligence*, 25(2), 1437-1449.
- Rezania, M. and Javadi, A. A. (2007). A New Genetic Programming Model for Predicting Settlement of Shallow Foundations. *Canadian Geotechnical Journal*, 44(12), 1462-1473.
- Roser, J. and Gosar. A., (2010). Determination of VS30 for Seismic Ground Classification in Ljubljana Area, Slovenia. *Geotechnica Slovenia*, 1(2), 61-67.

- Roy, N. and Sahu, R.B. (2012). Site Specific Ground Motion Simulation and Seismic Response Analysis for Microzonation of Kolkata. *Geomechanics and Engineering*, 4(1), 1-18.
- Sawafa, S. (2004). A Simplified Equation to Approximate Natural Period of Layered Ground on the Elastic Bedrock for Seismic Design of Structures. *Proceeding of the 13th World Conference on Earthquake Engineering*, Vancouver, Canada, August.
- Seshunarayana, T. and Sundararajan, N. (2012). Determination of shear wave velocity and depth to basement using multichannel analysis of surface wave technique. *Journal of the Geological Society of India*, 80(4), 499–504.
- Shahnazari, H. Shahin and Tutunchian, M. (2013). Evolutionary-based approaches for settlement prediction of shallow foundations on cohesionless soils. *International Journal of Civil engineering*, **12**(1), 55-64.
- Smith, G.N. (1986). *Probability and Statistics in Civil Engineering*. Collins, London.
- Standard2800. (2014). Iranian Code of Practice for Seismic Resistant Design of Buildings, Permanent Committee for Revising the Iranian Code of Practice for Seismic Resistant Design of Buildings, Building and Housing Research Center; Tehran, Iran (In Persian).
- Street, R., Woolery., E., Wang, Z. and Harik, I. (1997). Soil classifications for estimating site-dependent response spectra and seismic coefficients for building code provisions in western Kentucky. *Engineering Geology*, 46(3), 331-347.
- Trifunac, M. (2016). Site conditions and earthquake ground motion – A review. *Soil Dynamics and Earthquake Engineering*, 90(1), 88-100.
- UBC97 (1997). *Uniform Building Code*, International Council of Building Officials; California, U.S.A.
- Vijayendra, K.V., Nayak. S. and Prasad, S. K. (2015). An Alternative Method to Estimate Fundamental Period of Layered Soil Deposit. *Indian Geotechnical Journal*, 45(2), 192-199.



**Masoud Motalebian** is a PhD candidate in Geotechnical Engineering, University of Islamic Azad University, Science and Research Branch, Tehran, Iran. He is a researcher in Civil Engineering field. He is interested in Geotechnical Engineering.



**Professor Dr. Masoud Hajjalilue Bonab** is Professor at Faculty of Civil Engineering, University of Tabriz, Iran. He holds a PhD degree in Geotechnical Engineering from University of Caen, Laboratoire Central des Ponts et Chaussées (LCPC), France. His research is Computational Geomechanics, Soil Engineering Behaviors, Soil-Cement, and Applications in Civil Engineering.



**Dr. Mohammad Davoudi** is an Assistant Professor of Geotechnical Engineering Research Center, International Institute of Earthquake Engineering and Seismology, Iran. He has a PhD degree in Geotechnical Earthquake Engineering, International Institute of Earthquake Engineering and Seismology, Iran. He is interested in Foundation Engineering & Geotechnical Structures.